

8066744

# 3rd International Symposium on High Voltage Engineering

**VOLUME 1**



TM8-2

H1

1979 X X

V.1



8066744

ASSOCIAZIONE ELETTROTECNICA  
ED ELETTRONICA ITALIANA

TM8-53  
H 63812

1979

V.1

# THIRD INTERNATIONAL SYMPOSIUM ON HIGH VOLTAGE ENGINEERING



E8066744

MILAN

28 - 31 AUGUST 1979

CENTRO CONGRESSI

LEONARDO DA VINCI



With the Cooperation of

**EUREL**

Convention of National Societies of  
Electrical Engineers of Western Europe



INSTITUTION OF ELECTRICAL AND  
ELECTRONICS ENGINEERS

North Italy Section



# VOLUME 1

## 11 - ELECTRIC FIELD CALCULATIONS

Special Reporter : H. Steinbigler (Federal Republic of Germany)

11.00 H. Steinbigler (Federal Republic of Germany)  
Special Report of Group 11

11.01 D. Utmischi (Federal Republic of Germany)  
Charge substitution method for three-dimensional high voltage fields.

11.02 E.U. Landers (Federal Republic of Germany)  
Computation of asymmetric, three-dimensional electric fields with any input conditions.

11.03 S. Sato, S. Menju, K. Aoyagi, M. Honda (Japan)  
Electric field calculation in 2 dimensional multiple dielectric by the use of elliptic cylinder charge.

11.04 S. Satyanarayana, K. Natarajan (India)  
An improved procedure for computation of electric fields in unbounded axisymmetric regions by boundary relaxation.

11.05 H. Okubo, M. Honda, S. Menju (Japan)  
Calculation error and the field discretization of finite element method.

11.06 H. Singer (Federal Republic of Germany)  
Computation of optimized electrode geometries.

11.07 S. Sato, S. Menju, T. Sakakibara, K. Aoyagi, M. Honda (Japan)  
Electric field calculation by charge simulation method using axispheroidal charge.

11.08 F. Lattarulo, G. Mastronardi (Italy)  
A finite element program applied to high voltage studies by use of minicomputer.

11.09 S. Kato (Japan)  
An estimation method for the electric field error of a charge simulation method.

11.10 J.M. Janiszewski, G. Gambirasio (Brasil)  
Improved finite element method for static electromagnetic field mapping.

11.11 H. Steinbigler (Federal Republic of Germany)  
Combined application of finite element method and charge simulation method for the computation of electric fields.

11.12 D. Metz (Federal Republic of Germany)  
Optimization of high voltage fields.

11.13 H. Okubo, M. Ikeda, M. Honda (Japan)  
Combination method for electric field calculation.

11.14 J.H. Mc Whirter, J.J. Oravec (USA)  
Three-dimensional electrostatic field solutions in a rod gap by a Fredholm integral equation.

11.15 Y.L. Chow, K.D. Srivastava, C. Charalambous (Canada)  
Field computation around a charged conducting sphere near a dielectric coated conducting plate and under a uniform external electric field.

11.16 H. Okubo, T. Amemiya, M. Honda (Japan)  
Borda's profile and electric field optimization by using charge simulation method.

11.17 A. Veverka (Czechoslovakia)  
Electrical field with space charge.

11.18 I. Ohshima, Y. Maikawa, T. Hamano, O. Sakakura, M. Honda (Japan)  
HVDC field characteristics with and without ac superposed in converter transformers.

11.19 I.P. Vereshchagin, V.E. Litvinov (USSR)  
Methods for calculating the electric field of a unipolar corona discharge.

11.20 P.N. Nikolopoulos (Greece)  
Evaluation of the electric field and of the field-lines of a 2-conductors-ground configuration.

11.21 P. Weiss (Federal Republic of Germany)  
Fictitious peaks and edges in electric fields.

11.22 F. Donazzi, G. Bianchi (Italy)  
Electrical field calculation in HVDC cable accessories.

11.23 C.M. Cooke, W.W. Heil (USA)  
An evaluation of iterative procedures employed in electric field calculations.

11.24 R. Wilkins, J.J. Little (United Kingdom)  
Computation of electric fields using the sander-function method.

## 12 - ELECTRIC FIELD MEASUREMENTS AND APPLICATIONS

Special Reporter : L.E. Zaffanella (USA)

12.00 L.E. Zaffanella (USA)  
Special Report of Group 12.

12.01 T. Takuma, T. Kawamoto (Japan)  
Field calculation including surface resistance by charge simulation method.

12.02 L.S. Palma, S.R. Naidu (Brasil)  
Electric field distortions due to free conducting particles in a uniform field.

12.03 I.A. Stathopoulos (Greece)  
Three-electrode systems on DC electric field.

12.04 P. Canadas, J. Dupuy, G. Schreiber (France) - T. Rickard, E. Selim, R. Waters (United Kingdom)  
Field and current density in a non-cylindrical coaxial system.

12.05 B. Bachmann (Switzerland)  
Models for computation mixed fields with the charge method.

12.06 S.M. Sadović (Yugoslavia)  
Numerical considerations of the effect of resistive coatings and surface pollution on the potential distribution of high-voltage insulating systems.

**12.07 J.P. Reilly (USA)**

An approach to the realistic-case analysis of electric field induction from AC transmission lines.

**12.08 Z. Haznadar, S. Milojkovic, I. Kamenica (Yugoslavia)**

Numerical field calculation of insulator chains for high voltage transmission lines.

**12.09 W. Focke (Federal Republic of Germany)**

The influence of the electric field on the behaviour of series connected insulating gaps with linear voltage distribution.

**12.10 F. Lattarulo, G. Mastronardi (Italy)**

Computation of fundamental electrical parameters applied to 50 Hz high electric and magnetic fields involving man.

**12.11 S. Kato, H. Kokai, Y. Nakajima, T. Kouno (Japan)**

Finite element method for the calculation of potential distribution to the porcelain insulator with semiconducting surface layer.

**12.12 M. Groszko, A. Szendzielorz (Poland)**

Distribution of electric field intensity under UHV overhead power lines in respect to "Track over track" shielding.

**12.13 Y. Chang, Y. Fei-Yu (China)**

The measurement and model of electrostatic induction in high voltage substations.

**12.14 J. Arciszewski, R. Kosztaluk (Poland)**

Electric field measurements in EHV overhead power systems.

**12.15 J.L. Lilien, P. Pirotte (Belgium)**

Transmission line conductor surface voltage gradients. Comparison between Mangoldt's and charge simulation methods.

**12.16 M. Akazaki, M. Hara (Japan)**

Distribution of electric field and ion current at ground level in smooth conductor-plane geometry.

**12.17 G. Molinari, G. Sciutto, A. Viviani (Italy)**

Experimental results and computer simulation of electric fields around insulating structures under AC and DC conditions.

**12.18 O. Nigol (Canada)**

Development and testing of corona-free high voltage line and station hardware.

**12.19 A. Nourai, L.E. Zaffanella, T.S. Lauber (USA)**

Audible and radio noise of toroidal grading rings in wet weather.

**12.20 R. Conti, A. Previ (Italy)**

Method for the calculation of the voltage and the current induced on metallic bodies close to ground under UHV overhead lines. Comparison with on-the-spot measurements.

**12.21 R. Conti, A. Previ (Italy)**

Study, design and construction, in a laboratory, of a system for submitting small animals to high electric fields at 50 Hz.

**12.22 A. Augugliaro, P. Buccheri, E. Carreca, L. Dusonchet (Italy)**

A computer-aided analysis of electrical fields of overhead conductors. Application to EHV and UHV lines and substations structures.

## **21 - DIELECTRIC STRENGTH OF SOLID INSULATION. TREEING**

Special Reporter : H. Kärner (Federal Republic of Germany)

**21.00 H. Kärner (Federal Republic of Germany)**

Special Report of Group 21.

**21.01 H. Matsuba (Japan)**

Conduction and treeing of polymers at the divergent field from a needle tip.

**21.02 W. Mosch, M. Eberhardt, R. Köppe, A. Georgi (German Democratic Republic)**

On the application of life time characteristics measured at model insulations to technical epoxy resin insulations.

**21.03 L. C. Thanh (Australia)**

A model for the electric breakdown in porous dielectric.

**21.04 S. Zoledziowski, J. H. Calderwood (United Kingdom) - S. Sakata, Y. Shibuya (Japan)**

Study of electrical treeing in epoxy resins using electro optical methods.

**21.05 M. Ieda, M. Nagao, M. Hikita, G. Sawa (Japan)**

Dielectric breakdown of high temperature polymers.

**21.06 J. Salge, M. Schaefer (Federal Republic of Germany)**

Thermally stressed electrical insulators at temperatures up to 1300 K.

**21.07 J. Agterberg, B.C. Koolhaas (the Netherlands)**

Investigation of an epoxy-resin insulator in SF<sub>6</sub>-gas for a 420 kV metal-clad substation.

**21.08 H. Wagner, W. Götz (Federal Republic of Germany)**

Investigations on electrical treeing in high voltage insulation materials.

**21.09 M. Nawata, H. Kawamura, M. Ieda (Japan)**

Treeing breakdown phenomena associated with space charge formation in ethylene-vinyl acetate copolymer.

**21.10 H. Mitsui, T. Yoshimitsu, Y. Mizutani, K. Umemoto (Japan)**

Electrical failure properties of cast epoxy resins.

**21.11 P. F. Mohr (Switzerland)**

Space charge measurements on PE samples under electrical stress.

**21.12 E.F. Peschke, W. Kalkner, G. Schroeder (F.R.G. of Germany)**

Impulse voltage strength of PE and XLPE insulations.

**21.13 K.B. Müller, W.D. Schuppe (Federal Republic of Germany)**

The behaviour of XLPE cables at extremely thermal stress depending on time.

**21.14 R. Patsch (Federal Republic of Germany)**

On the growth-rate of trees in polymers.

**21.15 V. Scuka, G. Nelin, H. Ryzko (Sweden)**

AC breakdown of XLPE cables prestressed with DC or VLF voltages.

**21.16 G. Pattini, L. Simoni (Italy)**

Discussion on the endurance tests with combined stress.

**21.17 G. Coletti (Italy), A. Sierota (Poland)**

Study of degradation processes in epoxy resin submitted to artificial void tests and to needle tests.

**21.18 L. Thione, R. Bucciatti, D. Perinelli, E. Sesto, G. Botta (Italy)**

An approach to the evaluation of the dielectric strength of extruded solid insulation.



## 22 - MACHINE INSULATION AND PARTIAL DISCHARGES

Special Reporter : L. Centurioni (Italy)

22.00 L. Centurioni (Italy)  
Special Report of Group 22.

22.01 S. Shihab (Australia)  
Partial discharges in solid insulation under high direct voltages.

22.02 H. Kärner, W. Kodoll (Federal Republic of Germany)  
The resistivity of solid insulating materials against internal partial discharges.

22.03 J. Hiley, O. A. El Gendy (United Kingdom)  
A comparison of the discharge resistance of epoxy resins.

22.04 A. Sultan, F. Sultan (Egypt)  
Effect of pulse voltage, temperature and humidity on lifetime and amount of partial discharge for some solid insulating films.

22.05 J. P. Reynders (South Africa)  
Partial discharges pulse shape analysis - a diagnostic tool.

22.06 H. Fuchs (Switzerland)  
GRP laminates and their use in heavy electrical engineering.

22.07 J. R. Laghari, A. H. Qureshi (Canada)  
Effects of partial discharges on synthetic insulation materials in air and other gases.

22.08 E. Koyanagi, K. Umemoto, S. Kenjo, Y. Tanaka (Japan)  
Deterioration of molding insulations due to internal partial discharge.

22.09 A. Leschanz, G. Praxl, H. Egger (Austria)  
The long-term voltage endurance of insulation specimens after electrical prestress.

22.10 H. Egger, G. Praxl (Austria)  
The behaviour of anti discharge coating of generator winding insulation exposed to high humidity.

22.11 W. H. Zwicknagl (Austria)  
On the problem of the influence of periodical overvoltage-tests on the life-time of generator winding insulation.

22.12 H. G. Kranz (Federal Republic of Germany)  
The influence on partial discharge behaviour of polyethylene test samples concerning cross-linking procedure.

22.13 I. J. Kemp, W. K. Hogg (United Kingdom)  
Fundamental study of impulse discharge breakdown at a gas-solid interface.

22.14 G. Lottanti, W. Striffeler, A. Piur (Switzerland)  
Components for the manufacture of stator windings insulation.

## 23 - LIQUID, IMPREGNATED, AND OUTDOOR ORGANIC INSULATION

Special Reporter : E. Woschnagg (Austria)

23.00 E. Woschnagg (Austria)  
Special Report of Group 23.

23.01 A. El-Arabaty, E. Mansour, S. El-Debeiky, M. A. El-Koshairy, E. A. Aly, A. E. Abdullah (Egypt)  
Aging of HV epoxy resin insulators under service conditions and its effects on their electrical characteristics.

23.02 K. Herstad, P. Soelberg, R. F. Svendsen (Norway)  
The generation of surface charges on polymer insulation and their influence on impulse voltage tests.

23.03 R. Von Olshausen, H. Westerholt (Fed. Rep. of Germany)  
Dielectric strength of SF<sub>6</sub>-impregnated polyethylene test samples under homogeneous AC stress.

23.04 J. Hiley, O. A. El-Gendy (United Kingdom)  
Dielectric breakdown in helium and in helium-solid combinations.

23.05 R. Fournie, Y. Le Gall, J. Perret, P. Recoupe (France)  
Contribution to the study of the ageing of mineral insulating oils.

23.06 S. Yakov (Italy)  
A method for the experimental determination of the "equiprobabilistic volt-time curves" for partial discharge inception in oil-paper insulation.

23.07 F. Bachofen (Switzerland), H. Bläsing (F. R. of Germany)  
The influence of nitrogen on the breakdown voltage of liquid SF<sub>6</sub>.

23.08 E. Steinort (Austria)  
Surface defects of filled epoxy resins caused by irradiation and partial discharge stress.

23.09 H. Kärner, D. Schulte, H. Wehinger (Fed. Rep. of Germany)  
Tracking and erosion of polymeric insulating materials for outdoor application.

23.10 A. Denat, B. Gosse, J. P. Gosse (France)  
Electrochemical decomposition of sulphur hexafluoride and transformer oil.

23.11 Yu. Torshin, O. A. Sinkevich (USSR)  
Electrical conduction and breakdown in liquid sulphur hexafluoride under the condition of below and above critical pressure.

23.12 A. A. Panov, B. A. Turkot, M. A. Oushev (USSR)  
Surface discharge and breakdown of multilayer insulation in liquid nitrogen.

23.13 A. G. Arson (USSR)  
Electric strength of film insulation in SF<sub>6</sub>.

23.14 H. Okubo, M. Ikeda, M. Honda, S. Menju (Japan)  
Electrostatic discharges in insulating oil.

23.15 I. P. Kulikov, J. S. Pintal, S. M. Shahgedarova (USSR)  
Investigation of low-intensity partial discharges in oil-paper insulation in slightly-distorted electric field.

23.16 J. F. Watson, J. H. Mason, A. C. Lynch (United Kingdom)  
Assessing materials for use as outdoor insulation.

23.17 E. O. Forster, P. P. Wong (USA)  
The dynamics of electrical breakdown in liquid hydrocarbons III.

23.18 M. Ikeda, T. Inoue (Japan)  
Statistical approach to breakdown stress of transformer insulation.

23.19 D. Baumann, K. Munk, H. Rembold (Switzerland)  
New laboratory results about the erosion resistance of epoxy casting systems and their significance for the outdoor weathering resistance.

23.20 P. Molfino, G. Molinari, A. Viviani (Italy)  
Theoretical and experimental investigation of impurity particle motion in solid-fluid insulating systems.

23.21 R. Wimmershoff (Federal Republic of Germany)  
Termination of a DC bulk power cable with superconductors.

23.22 A. Marconcini, G. Picci, G. Villa (Italy)  
Behaviour of paper impregnated with SF<sub>6</sub>.

23.23 Th. Praehauser (Switzerland)  
Ageing test for hydrocarbon-impregnated kraftpaper-insulation.

## 31 - SF<sub>6</sub>, OTHER GASES (except air) AND VACUUM. PHYSICAL APPROACH.

Special Reporter : O. Farish (United Kingdom)

31.00 O. Farish (United Kingdom)  
Special Report of Group 31.

31.01 W. Pfeiffer, W. Schmitz (Federal Republic of Germany)  
Experimental and theoretical investigation of streamer discharge in SF<sub>6</sub>.

31.02 J. Juchniewicz, B. Mazurek, A. Tyman (Poland)  
On some size effects of high voltage vacuum insulation.

31.03 N.H. Malik, A.H. Qureshi (Canada)  
Non-uniform field breakdown in SF<sub>6</sub> and its mixtures with helium and nitrogen.

31.04 H. Korge, K. Kudu, M. Laan (USSR)  
The discharge in pure nitrogen at atmospheric pressure in point-to-plane discharge gap.

31.05 K.P. Brand, J. Kopainsky (Switzerland)  
Model description of breakdown properties for unitary electro-negative gases and gas mixtures.

31.06 G. Dreger (Federal Republic of Germany)  
The influence of the rate of primary electrons on the delay of firing at breakdown of impulse voltage in SF<sub>6</sub> at uniform and inhomogeneous fields.

31.07 P.A. Chatterton (USA)  
A model for the breakdown of SF<sub>6</sub> in the presence of positive impulse corona.

31.08 M. Abdel-Salam, W. Taschner (Fed. Rep. of Germany)  
On the corona pulse randomness in compressed SF<sub>6</sub>.

31.09 B. D. Schmidt (Federal Republic of Germany)  
AC breakdown of vacuum gaps at high voltages.

31.10 A.H. Cookson, B.O. Pedersen (USA)  
Analysis of the high voltage breakdown results for mixtures of SF<sub>6</sub> with CO<sub>2</sub>, N<sub>2</sub> and air.

31.11 W. Knorr (Federal Republic of Germany)  
A model to describe the ignition time-lag of slightly nonuniform arrangements in SF<sub>6</sub>.

31.12 Th. Aschwanden (Switzerland)  
Ionization and attachment coefficients in SF<sub>6</sub>/N<sub>2</sub>-mixtures.

31.13 W. Voss (Federal Republic of Germany)  
Discharge development of non-uniform gaps in SF<sub>6</sub>-N<sub>2</sub> gas mixtures.

31.14 E. Gockenbach, A. Wieland (Federal Republic of Germany)  
The breakdown behaviour of some electronegative gases and gas mixtures.

31.15 O. Farish, O.E. Ibrahim, A. Kurimoto (United Kingdom)  
Prebreakdown corona processes in SF<sub>6</sub> and SF<sub>6</sub>/N<sub>2</sub> mixtures.

31.16 J.M. Pelletier, Y. Gervais, D. Mukhedkar (Canada)  
Dielectric strength of N<sub>2</sub>-He mixtures and comparison with N<sub>2</sub>-SF<sub>6</sub> and CO<sub>2</sub>-SF<sub>6</sub> mixtures.

## 32 - SF<sub>6</sub>, OTHER GASES (except air) AND VACUUM. ENGINEERING APPROACH.

Special Reporter : S. Rusck (Sweden)

32.00 S. Rusck (Sweden)  
Special Report of Group 32.

32.01 W. Mosch, W. Hauschild, J. Speck, S. Schierig (German Democratic Republic)  
Phenomena in SF<sub>6</sub> insulations with particles and their technical valuation.

32.02 H. Lau, H. Schultz (Federal Republic of Germany)  
Times to breakdown in SF<sub>6</sub> at high pressures.

32.03 B. Blankenburg (Federal Republic of Germany)  
Flashover behaviour of cylindrical insulators in SF<sub>6</sub>, N<sub>2</sub> and SF<sub>6</sub>-N<sub>2</sub>-mixtures.

32.04 H. Kärner, H.J. Voss (Federal Republic of Germany)  
The particle influenced breakdown of insulating surfaces in SF<sub>6</sub> under oscillating switching impulse voltage.

32.05 H. Bläsing (F.R. of Germany), R. Thaler (Switzerland)  
Breakdown of SF<sub>6</sub> with drops of liquid SF<sub>6</sub>.

32.06 S. Vibholm, A. Pedersen, J. M. Christensen, P. Thyregod (Denmark)  
The effect of surface roughness on low probability first breakdown in compressed SF<sub>6</sub>.

32.07 R. Moll, E. Schade (Switzerland)  
Investigation of the dielectric recovery of SF<sub>6</sub>-blown high-voltage switchgear arcs.

32.08 A.E. Vlastós, S. Rusck (Sweden)  
Influence of electrode coating on the impulse breakdown of SF<sub>6</sub>.

32.09 H. Dietz, M. Ermel (Federal Republic of Germany)  
A condenser bushing with SF<sub>6</sub>-impregnated plastic film insulation.

32.10 S.J. Dale, R.E. Wootton (USA)  
Effect of fixed particle protrusions on 60 Hz and impulse breakdown voltage-pressure characteristics in SF<sub>6</sub>.

32.11 I.M. Bortnik, V.P. Vertikov (USSR)  
Discharge development in SF<sub>6</sub>.

32.12 A. Schei, T. Henriksen, A. Rein (Norway)  
Withstand characteristics and breakdown criteria of SF<sub>6</sub>-insulation.

32.13 I.C. Somerville, D.J. Tedford (United Kingdom)  
Breakdown in high-pressure SF<sub>6</sub> between small sphere electrodes.

32.14 H.M. Ryan (United Kingdom)  
Further breakdown characteristics in SF<sub>6</sub> and air.

32.15 C. Masetti, B. Parmigiani (Italy)  
Area effect on the electrical breakdown of compressed SF<sub>6</sub>-insulated systems.

32.16 Y. Shibuya, K. Nakanishi, M. Yasuda, T. Nitta (Japan)  
An improved method of field analysis and its application to the insulation design of gas insulated systems.

32.17 J. Donon, J. Vigreux (France)  
Partial discharge detection and measurements in compressed SF<sub>6</sub> at high electric fields.



# THIRD INTERNATIONAL SYMPOSIUM ON HIGH VOLTAGE ENGINEERING

MILAN 28-31 AUGUST 1979

11.00

## ELECTRIC FIELD CALCULATION

Special Report of Group 11

by

H. STEINBIGLER

Technische Universität München

Munich, West Germany

### REVIEW

The 22 papers in group 11 may be divided into the following 4 subjects:

Subject 1: Finite element method (FEM) and finite difference method (FDM);

Subject 2: Integral methods including charge simulation method (CSM) and the combination of CSM and FEM;

Subject 3: Optimization of high voltage insulation systems by means of electric field calculation;

Subject 4: Special field calculation problems: electric fields with space charges and dielectric effects.

Subject 1 - The papers to this subject deal with

the application of FEM on field problems with non-linear resistivities in HVDC design (11.18, 11.22),

the solution of three-dimensional problems (11.10) and

the application of FDM on problems with unbounded regions by means of boundary relaxation (11.04).

A new way of grid refinement for two-dimensional and axi-symmetrical fields is shown in Paper 11.05, where the relationship between the number of elements and the accuracy of the calculation is also treated. An important question with respect to the application of field calculation in high voltage practice is the subject of Paper 11.08: the improvement of FEM for the use of minicomputers.

Subject 2 - The contributions to CSM show some emphasis on the introduction of new types of charges and on the optimum location of these charges in order to reduce the size of the equation systems and consequently the necessary amount of core storage (11.01, 11.02, 11.03, 11.07, 11.15). This reduction is of substantial importance particularly for the calculation of three-dimensional fields without symmetries. Besides point-charges and line- or ring-charges with constant or partially constant charge densities, the use of area-charges, volume-charges and dipoles is proposed. The application of a Fredholm integral equation corresponding to a double layer of charges on the boundary is presented also as a useful method for the solution of three-

dimensional electrostatic field problems (11.14).

The question of accuracy of CSM and the possibilities to check this accuracy are discussed in the Papers 11.07, 11.09 and - in connection with the calculation of a 2-conductors-ground arrangement - in Paper 11.20.

The discussions during ISH 1972 and 1975 concerning the advantages and disadvantages of FEM and CSM resulted in proposals for a combination of these methods (11.11, 11.13).

The electric field of a spherical charged particle near a dielectric-coated conducting plate is calculated in Paper 11.15 by means of Green's functions and an optimization algorithm based on least-squares method.

Subject 3 - The papers 11.06, 11.12 and 11.16 deal with the optimization of the geometry of high voltage insulation systems. The aim of this optimization are electrodes with an optimum field strength distribution along the maximum stressed parts of the electrode surface. Furthermore dependencies between electrode curvature and onset gradient can be introduced into this optimization process in order to get a maximum value of onset voltage (11.06). With respect to the strategy of the optimization, two possibilities are shown: an automatic procedure or an interactive calculation by means of a graphic terminal, where the optimization process can be controlled by the experience of the designer (11.12).

Subject 4 - In Paper 11.21 it is shown that numerical field computation can be successfully used to investigate dielectric arrangements especially in the region of dielectric edges or areas, where electrodes and dielectrics contact each other.

The calculation of electric fields with space charges is treated in the Papers 11.17 and 11.19. In Paper 11.17 an analytical solution for the electric field between a hyperboloidal cone and an earthed plane is shown, where the given space charge density distribution between the electrodes is not constant. Methods for the computation of the electric field of an unipolar corona discharge are discussed in Paper 11.19.

### QUESTIONS

Three-dimensional field without symmetry - Fortunately many electric field problems in high voltage engineering can be simulated by two-dimensional or axi-sym-



metrical arrangements. But there are still many cases where such a simulation is not possible, and a three-dimensional field problem without symmetry must be calculated. As the review of the presented papers shows, both methods - FEM (11.10) and integral methods (11.01, 11.02, 11.07, 11.14) - are used for such calculations.

#### QUESTION 1:

- a) In Paper 11.10 the subdivision of the grid by means of tetrahedrons is proposed for FEM. What is the experience with grid refinements in this way? Are there experiences with the use of elements of higher order for grid refinement? Is it possible to use the proposed grid refinement in Paper 11.05 in a modified way for the calculation of three-dimensional fields as well?
- b) Which experiences exist with the application of CSM for calculation of three-dimensional problems? Are there proposals to use integral methods for the calculation of three-dimensional fields with more dielectrics?

Equation systems - In FEM, FDM and CSM the spatial discretization finally results in a system of linear equations. For FEM these systems are solved in some cases by means of Gauß-elimination (11.11) or Cholesky-method (11.10). In other cases these equation systems are solved by iterative methods (11.04, 11.05, 11.08, 11.22).

#### QUESTION 2:

What is the experience with respect to the convergency of iterative methods, particularly if nonlinearities must be considered? Is the introduction of relaxation factors helpful?

Accuracy of field computation - The question of the accuracy of field computation is treated in the Papers 11.04, 11.05, 11.07, 11.09 and 11.20.

#### QUESTION 3:

- a) Which possibilities are available for the estimation of accuracy for FEM, FDM and integral methods?
- b) What is the accuracy of these methods for the calculation of conductive or dielectric peaks or edges as shown in Paper 11.21?
- c) What are the requirements of high voltage design practice, with respect to the accuracy of field computations?

Use of minicomputers - In Paper 11.08 a program on the basis of FEM is described for the use of minicomputers. In Paper 11.12 the question of application of table calculators for optimization is also raised.

#### QUESTION 4:

- a) Are there other activities using minicomputers for the calculation of more complicated electric field problems by means of FEM, FDM or integral methods?
- b) An obstacle for the application of

minicomputers seems to be the size of the equation systems. Is it possible to reduce this size for CSM considerably by a proper selection and location of charges as shown in the Papers 11.07, 11.03 and 11.15, so that minicomputers can be applied?

Optimization methods - The Papers 11.06, 11.12 and 11.16 describe optimization methods working automatically. In Paper 11.12 an interactive way of optimization by means of a graphic terminal is mentioned.

#### QUESTION 5:

Which way of optimization promises to be more economic in high voltage practice: the interactive method, where the aid of an experienced engineer is necessary, or the automatic way which needs some amount of computation, particularly when more complicated systems must be optimized?

Electric fields with space charges - In the Papers 11.02, 11.17 and 11.19 the calculation of electric fields with space charges is treated. It seems that the calculation of such fields is possible - even analytically - when the space charge distribution is known. But in connection with the calculation of discharge this distribution is unknown. It depends from the field strength distribution itself, and for its determination the physical laws of discharge must be considered.

#### QUESTION 6:

Is there sufficient knowledge of physical data for the calculation of electric fields with space charges, especially with respect to the investigation of breakdown or corona discharge? How can the statistic behavior of discharge phenomena be introduced into the field calculation?

Requirements with respect to computer programs - Within the last 10 years there was a considerable progress in the development of computer programs for the computation of electric and magnetic fields in high voltage engineering. Parallel to this development there was a significant decrease of specific costs for core storage and computation time, and this trend seems to continue in future. This development stimulates again the following general question, already discussed during ISH 1972 and 1975.

#### QUESTION 7:

Which requirements are set up by the designer of high voltage apparatus or by research engineers with respect to computer programs for field calculation? What can be done in future in order to give a better help for high voltage practice, e.g. with respect to the data input and the handling of such programs?

## Charge Substitution Method for Three-Dimensional High Voltage Fields

D. Utmischi

Technical University Munich, (F.R. of Germany)

### 1. Abstract

This report presents a method for the calculation of three-dimensional and unsymmetrical electric fields basing on the charge simulation method. In opposition to the known methods point charges in combination with line and ring charges with sectorial constant charge density are introduced. A suitable transformation of the co-ordinates enables the superposition by means of these charges. With this modification any three-dimensional field arrangement can be calculated. This method will be demonstrated with a practical example.

### 2. Introduction

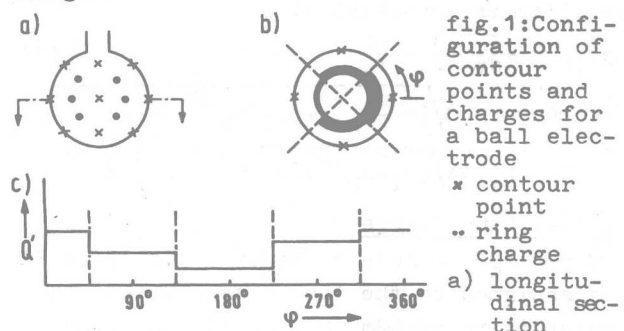
For high voltage testing in a laboratory the electrode system can be imitated only conditionally. Here the influence of additional electrodes, of transformers, voltage feed lines and grounded parts on the distribution of field intensity and of potential shall also be dealt with, and the minimum distance for correct testing shall be determined. These arrangement ordinarily represent a three-dimensional unsymmetric case.

### 3. Method of calculation

The method of calculating three-dimensional field arrangements published so far [4] started from fictive line and ring charges distributed in the shape of a periodic function. In this connection it is necessary that each single electrode is rotationally symmetrical. The distribution of charge that has to be determined is divided into its constant part and its portion of harmonic waves almost analogous to a Fourier analysis.

In opposition to that, in this treatise fictive line and ring charges with sectorially constant charge density will be introduced,

whereby a symmetry of rotation is no more necessary. The ring charges are segmented at random and the charge density is maintained constant in the area of each segment by means of which ring segment charges develop. To illustrate this method figure 1 shows a longitudinal section across a ball electrode. For reasons of a well-ordered arrangement only three ring charges are scheduled for the simulation of the electrode contour. Any ring charge of that kind consists in this case of four ring segment charges to whom in turn practically four contour points on the electrode surface are assigned.



b) vision at a ring charge with sectorially constant charge density (4 ring segment charges) c) unrolling this ring charge

Each line and ring charge inclusive of their mirror charges will be assigned to a Cartesian co-ordinate system of its own and at each stage of computation a co-ordinate transformation will be conducted for the complete arrangement; this transformation of co-ordinates provides for a geometrical turn and displacement so that the field arrangement as such remains untouched. By the aid of this transformation of co-ordinates it is now possible to distribute line and ring charges in space at random.

#### 3.1. Potentials and Field Intensities

The principal equation of charge substit-

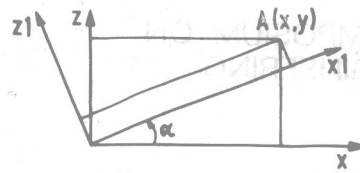
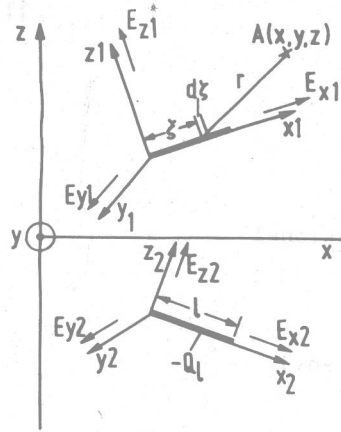
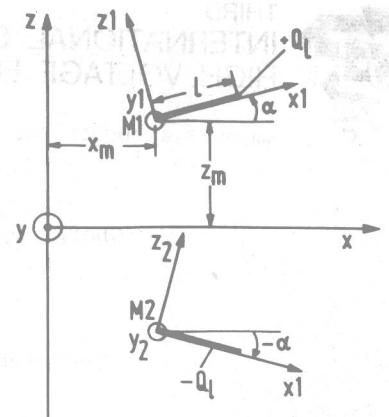


figure 2

figure 3

figure 4



tion method can be taken from /1-6/:

$$\mathbf{P} \cdot \mathbf{q} = \mathbf{u} \quad (1)$$

whereby  $\mathbf{P}$ : potential coefficient matrix

$\mathbf{q}$ : one-column charge matrix(unknown)

$\mathbf{u}$ : one-column potential matrix(known)

The electric field intensity  $\vec{E}$  is the negative gradient of the potential  $\phi$ , and here-with for its x-, y- and z-components applies:

$$E_x = -\frac{\partial \phi}{\partial x}; E_y = -\frac{\partial \phi}{\partial y}; E_z = -\frac{\partial \phi}{\partial z} \quad (2)$$

### 3.1.1. Point Charge

For the potential of a point charge  $Q(x, y, z)$  (index k) referring to charge and its mirror charge for a point  $A(x, y, z)$  (index i) applies the expression:

$$P_{i,k} = \frac{1}{4\pi\epsilon} \left( \frac{1}{r} - \frac{1}{r_s} \right) \quad (3)$$

whereby  $r = \sqrt{(x_i - x_k)^2 + (y_i - y_k)^2 + (z_i - z_k)^2}$

$$r_s = \sqrt{(x_i - x_k)^2 + (y_i - y_k)^2 + (z_i + z_k)^2}$$

### 3.1.2. Line Charge

If the co-ordinate system  $(x_1, y_1, z_1)$  (fig.2) is assigned to the line charge  $Q_1$  and the co-ordinate system  $(x_2, y_2, z_2)$  is assigned to the mirror charge  $-Q_1$ , then each element  $df$  of the line charge has the charge:

$$dQ = \frac{Q_1}{l} df \quad (4)$$

For the potential referred to the charge in an arbitrary point  $A(x, y, z)$  applies:

$$dp_{i,k} = \frac{1}{4\pi\epsilon} \frac{df}{r} \quad (5)$$

Thus the potential in point A with the order i is found, caused by the charge k, by integration over the charge length l:

$$P_{i,k} = \frac{1}{4\pi\epsilon l} \ln \left\{ \frac{[1 - x_1 + \sqrt{z_1^2 + y_1^2 + (1 - x_1)^2}]}{[-x_1 + \sqrt{x_1^2 + y_1^2 + z_1^2}]} \cdot \frac{[-x_2 + \sqrt{x_2^2 + y_2^2 + z_2^2}]}{[1 - x_2 + \sqrt{z_2^2 + y_2^2 + (1 - x_2)^2}]} \right\} \quad (6)$$

The new co-ordinates  $x_1$  and  $z_1$  are defined according to fig.3:

$$\begin{aligned} x_1 &= x \cos \alpha + z \sin \alpha \\ z_1 &= -x \sin \alpha + z \cos \alpha \end{aligned} \quad (7)$$

If this coordinate transformation is applied to the line charge  $Q_1$  and its mirror charge  $-Q_1$  we get the following for the new co-ordinates  $A(x_1, y_1, z_1)$  and  $A(x_2, y_2, z_2)$  according to fig. 4:

$$\begin{aligned} x_1 &= (x - x_m) \cos \alpha + (z - z_m) \sin \alpha \\ y_1 &= y - y_m \\ z_1 &= -(x - x_m) \sin \alpha + (z - z_m) \cos \alpha \\ x_2 &= (x - x_m) \cos \alpha - (z + z_m) \sin \alpha \\ y_2 &= y - y_m \\ z_2 &= (x - x_m) \sin \alpha + (z + z_m) \cos \alpha \end{aligned} \quad (8)$$

This co-ordinate transformation provides for a displacement of the origin of co-ordinates into point  $M_1$  and  $M_2$  resp. and a turn round angle  $\alpha$  and  $-\alpha$  resp. in the x-z-plane.

In the x-z-plane charge  $Q_1$  is twisted by  $\alpha$ , whereas the charge mirrored in the x-y-plane is twisted by  $-\alpha$ . That is the reason why a negative sign occurs with the  $\sin \alpha$ -terms in the co-ordinate system of the mirror charge.

In the three-dimensional transformation of co-ordinate systems there must be in addition to the displacement of the x-, y-, z-co-ordinates provided for a double turn. The first turn happened in the x-z-plane (fig.4), the second turn of the co-ordinate systems of charge  $Q_1$  and its mirror charge  $-Q_1$  by angle  $\beta$  is necessary in the x-y-plane.

Hence we receive the following co-ordinates:

$$\begin{aligned} x_1 &= [(x - x_m) \cos \beta + (y - y_m) \sin \beta] \cos \alpha + (z - z_m) \sin \alpha \\ y_1 &= -(x - x_m) \sin \beta + (y - y_m) \cos \beta \\ z_1 &= [(x - x_m) \cos \beta + (y - y_m) \sin \beta] \sin \alpha - (z - z_m) \cos \alpha \end{aligned} \quad (9)$$



$$\begin{aligned}x_2 &= [(x-x_m)\cos\beta + (y-y_m)\sin\beta]\cos\alpha - (z+z_m)\sin\alpha \\y_2 &= -(x-x_m)\sin\beta + (y-y_m)\cos\beta \\z_2 &= [(x-x_m)\cos\beta + (y-y_m)\sin\beta]\sin\alpha + (z+z_m)\cos\alpha\end{aligned}$$

For reasons of clearness it is to be mentioned that line charge  $Q_1$  and its mirror charge are turned in equal direction in the x-y-plane by angle  $\beta$ , which results in no change of sign of the  $\sin\beta$ -terms.

The components of field intensity are derived from equation (2). The differentiation of potential  $\phi$  in the co-ordinate systems  $(x_1, y_1, z_1)$  and  $(x_2, y_2, z_2)$  is conducted separately. Thus the  $x_1$ -,  $y_1$ - and  $z_1$ -components of the field intensity of charge  $Q_1$  in the co-ordinate system  $(x_1, y_1, z_1)$  are obtained, and the  $x_2$ -,  $y_2$ - and  $z_2$ -components of the field intensity of the mirror charge  $-Q_1$  in the co-ordinate system  $(x_2, y_2, z_2)$ . For the superposition of the field intensity components of charge  $Q_1$  and its mirror charge  $-Q_1$  the  $x_1$ -,  $y_1$ - and  $z_1$ -components as well as the  $x_2$ -,  $y_2$ - and  $z_2$ -components of the field intensity must be transformed back into the main co-ordinate system  $(x, y, z)$ .

The  $x_1$ -,  $y_1$ - and  $z_1$ -components of the field intensity of charge  $Q_1$  as well as the  $x_2$ -,  $y_2$ - and  $z_2$ -components of the mirror charge  $-Q_1$  are now with the angles  $\alpha$  and  $\beta$  and  $-\alpha$  and  $\beta$  resp. transformed back into the main co-ordinate system  $(x, y, z)$  and added vectorially. Thus the field intensity components of the charge  $Q_1$  and its mirror charge in the main co-ordinate system  $(x, y, z)$  result from:

$$\begin{aligned}E_{x1,k} &= (E_{x1i,k} + E_{x2i,k})\cos\alpha\cos\beta - (E_{y1i,k} + E_{y2i,k})\sin\beta - (E_{z1i,k} + E_{z2i,k})\sin\alpha\cos\beta \\E_{y1,k} &= (E_{x1i,k} + E_{x2i,k})\cos\alpha\sin\beta + (E_{y1i,k} + E_{y2i,k})\cos\beta - (E_{z1i,k} + E_{z2i,k})\sin\alpha\sin\beta \\E_{z1,k} &= (E_{x1i,k} + E_{x2i,k})\sin\alpha + (E_{z1i,k} + E_{z2i,k})\cdot\cos\alpha\end{aligned}\quad (10)$$

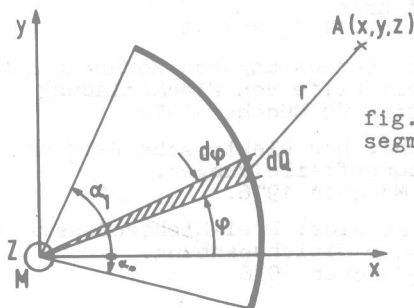


fig.5: Ring segment charge

### 2.1.3. Ring Charge

In an unsymmetric space arrangement the

ring charges have no constantly distributed charge density above their entire perimeter. It can, however, be assumed that the charge density remains constant within a certain angular range which is applied according to accuracy.

According to fig.5 each element of the ring segment charge carries the charge

$$dQ = \frac{Q}{(\alpha_1 - \alpha_0)} d\varphi \quad (11)$$

For the potential referred to the charge in an arbitrary point A(x,y,z) applies:

$$dp_{i,k} = \frac{1}{4\pi\epsilon(\alpha_1 - \alpha_0)} \frac{d\varphi}{r} \quad (12)$$

Thus the potential in a point A with order i, which is caused by charge k can be found by integration over the angle  $(\alpha_1 - \alpha_0)$ .

If the co-ordinate system  $(x_1, y_1, z_1)$  is assigned to charge Q and the co-ordinate system  $(x_2, y_2, z_2)$  to the mirror charge  $-Q_1$ , the potential referring to charge results in point A(x,y,z).

$$\begin{aligned}p_{i,k} &= \frac{1}{4\pi\epsilon(\alpha_1 - \alpha_0)} \int_{\alpha_0}^{\alpha_1} \frac{1}{\sqrt{x_1^2 + y_1^2 + z_1^2 + r_0^2 - 2x_1r_0\cos\varphi - 2y_1r_0\sin\varphi}} \\&\quad - \frac{1}{\sqrt{x_2^2 + y_2^2 + z_2^2 + r_0^2 - 2x_2r_0\cos\varphi - 2y_2r_0\sin\varphi}} d\varphi\end{aligned}\quad (13)$$

The field intensity components are derived from equation (2). The integrations should advisably be conducted numerically.

The new co-ordinates  $x_1, y_1, z_1$  and  $x_2, y_2, z_2$  are derived as from line charges. Point M  $(x_m, y_m, z_m)$  is the centre of ring charge. The field intensity components  $E_{x1i,k}$ ,  $E_{y1i,k}$ ,  $E_{z1i,k}$ ,  $E_{x2i,k}$ ,  $E_{y2i,k}$  and  $E_{z2i,k}$  must according to equation (10) be transformed back into the main co-ordinate system and added vectorially.

### 3.2. Control of Accuracy of Calculation

With the charge substitution method the accuracy of calculation can be controlled in three ways which are described more detailed in /1/:

1. Calculation of the spatial shape of the potential in the electrode range
2. Calculation of the spatial shape of field intensity in the electrode range
3. Formation of the second derivative of the potential

To keep the numerical calculation as clear as possible, only the first two methodes

should be made use of.

#### 4. Possibilities of Application

Any arbitrary three-dimensional field arrangement can in principle be calculated by the described method of calculation. In the following a survey of the different possibilities of application is given:

1. Calculation of electric fields in the range of high voltage overhead lines with regard to the tower and the sag of conductors and the differently formed metallic objects under the line /5/.
2. Calculation and optimization of arc protection armatures for high and ultra high voltage power systems.
3. Calculation of field stress of high voltage switches for encapsulated and outdoor systems.
4. Calculation of highly field-stressed parts of high voltage in high and ultra high voltage transformers.
5. Computation and dimensioning of electrical paint spraying systems.
6. Computation of missile-like objects in the field /6/.
7. Determination of the minimum separation for high voltage testing in a laboratory for a correct test.

#### 5. Example of Application

At the high voltage testing of a test object (double toroid) the testing of the maximum field intensity on this test object is to be determined as a function of the distance of a vertical live feed line as well as of a testing transformer. The equivalent circuit for the computation is shown in fig.6.

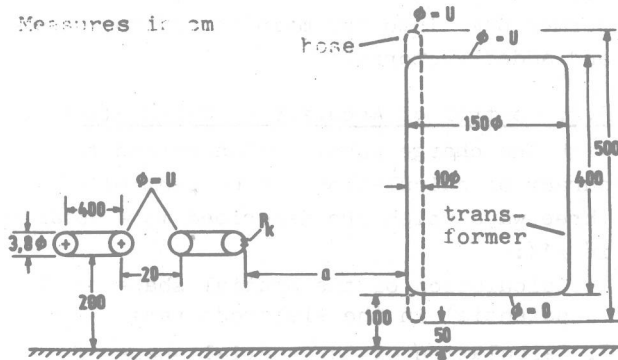


fig.6: Equivalent circuit for the calculation of feed line (hose) and transformer resp.

The distance of the double toroid to the ground amounts to 2m. The feed line (hose)

was imitated as a vertical, live cylinder with a diameter of 10 cm and a length of 5 m. The transformer was simulated as a cylinder with a diameter of 1.5 m and a length of 4m. The voltage distribution along the transformer was assumed linear.

Fig.7 shows (in%) the deviation of the maximum field intensity on the double toroid (point  $P_k$ ) as a function of distance  $a$ . Reference magnitude is the maximum field intensity without feed line and without transformer resp. The intersection of both curves in fig.7 can be explained by the fact that the supposed linear voltage distribution of the transformer makes itself felt

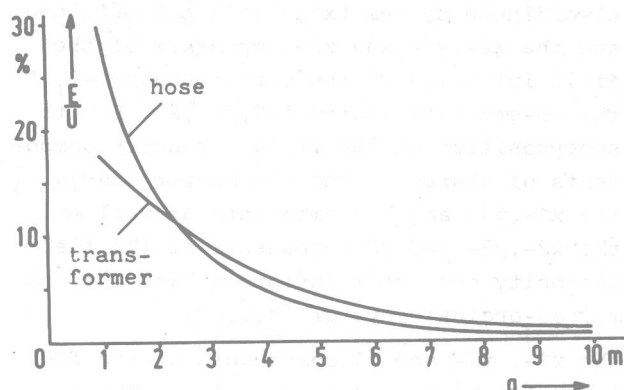


fig.7: Deviation of the maximum field intensity (in%) on the double toroid (point  $P_k$ ) as a function of distance  $a$  (reference magnitude is the maximum field intensity without transformer resp.)

to a greater extent with shorter distances  $a$  as against the spatially constant voltage of the feed line.

#### 6. References

- /1/ H. Steinbigler: Anfangsfeldstärken und Ausnutzungsfaktoren rotationssymmetrischer Elektrodenanordnungen in der Luft. Diss. TU München 1969
- /2/ P. Weiß: Berechnung von Zweistoffdielektrika. ETZ-A 90 (1969) S. 693-694.
- /3/ B. Bachmann: Freies Potential beim Ladungsverfahren. ETZ-A 94 (1973) S. 741-742.
- /4/ H. Singer: Berechnung von Hochspannungsfeldern mit Hilfe von Flächenladungen. Habilitation TU München 1974
- /5/ D. Utmischi: Das elektrische Feld unter Hochspannungsfreileitungen. Diss. TU München 1976.
- /6/ I.A. Stathopoulos: Drei-Elektrodensysteme bei hoher Gleichspannung. Diss. TU München 1978.



# THIRD INTERNATIONAL SYMPOSIUM ON HIGH VOLTAGE ENGINEERING

MILAN 28-31 AUGUST 1979

11.02

## COMPUTATION OF ASYMMETRIC, THREE-DIMENSIONAL ELECTRIC FIELDS WITH ANY INPUT CONDITIONS

E.U. Landers  
Hochschule der Bundeswehr  
München, West Germany

**Abstract** - A program based on the charge simulation method is presented, which allows the computation of asymmetric, three-dimensional electric fields. Because of its strong kit system any type of simulation charge and any input condition may be used. Real or complex values of the simulation charges (point-, line-, area- or volume type) allow calculation of DC and AC fields. Every input condition concerns either potentials or fieldstrengths or charges. At present of these three types of input conditions there are realized: fixed and free potentials (charged and uncharged electrodes), fixed fieldstrengths and various dielectrics, fixed charges. Limiting values of charge and fieldstrengths for an charging process of various formed particles in homogenous fields will be calculated as an example.

### INTRODUCTION

A powerful method for the numerical analysis of electric fields in the high-voltage technology is the simulation charge method. It has been designed in its originally form [1] for the analysis of rotation symmetric electrode arrangements in air. Point charges, finite line charges and ring charges were used with constant charge value. There was given a fixed potential as an input condition in the contour points on the electrode surface. From that a linear equation system was yielded (matrix of potential coefficients  $\times$  column matrix of unknown simulation charges = column matrix of unknown potentials) and the size of simulations charges was determined with it. By aid of the simulation charges, known then according to their value and spatial site, potential and fieldstrength could be determined in each point of the space between the electrodes. The simulation charge method has been extended in two different ways: The introduction of new input conditions allowed a calculation of rotation symmetric electrode arrangements with two different dielectrics [2] and the calculation of uncharged electrodes on a free potential [3]. New types of simulation charges raise the efficiency of the procedure: Line simulation charges with periodic charge density distribution allowed the calculation of grid electrodes [4] and three-dimensional arrangements out of single electrodes with rotation symmetry. Asymmetric threedimensional arrangements could be analysed by the introduction of line simulation charges divided in sections with constant charge density [5]. The use of simulation charges with complex values allowed also the calculation of electrode systems with dephased potentials [5]. Area charges [6] at last can be put in advantageously for the calculation of thin electrodes and boundary surfaces of dielectrics. In the paper in hand there will be described a program which permits any type of simulation charges and any input conditions because of its strong kit system.

### FUNDAMENTALS OF THE PROGRAM

A physically complete description of asymmetric three-dimensional electric fields is given by the spatial geometry of surfaces (electrode surfaces re-

spectively boundary surfaces of dielectrics) and by the charges, finely distributed on these surfaces or in the space. For any geometry, analytical not representable, it is necessary to discrete these physical arrangements to make them available for the numeric calculation. The complete geometry of boundary surfaces will be replaced by contour points and the finely distributed charges will be concentrated in simulation charges with constant values. For the determination of unknown simulations charges there will be set up in each contour point any physical condition, that can be related to potentials as well as to fieldstrengths or charges. After the solution of the equation system resulting from it, the simulation charges are known according to value and spatial site, so that potentials and fieldstrengths can be calculated in each point of the space. The physical dates will be exactly observed in the contour points (within the scope of calculating accuracy) whereas in other regions they are approximatively fulfilled. Any general or local improvement of the quality of the approximation is possible by adequate concentration of the contour points. The main problem in calculating asymmetric three-dimensional electric fields is, that any spatial allocation is possible between simulation charges and contour points. Therefore two auxiliary coordinates are used beside the cartesian main coordinates  $(X,Y,Z)$ : A system  $(XK,YK,ZK)$  referred to the respective contour point serves for the input of the geometry and for the formulation of input conditions, a system  $(XQ,YQ,ZQ)$  referred to the respective simulation charge is used when calculating results. The example of a finite line charge shows simplifications made possible by it: In the system  $(XK,YK,ZK)$  (Fig. 1) the line charge is always placed in the  $XK,YK$ -plane (symmetrically to the  $XK$ -axis and parallelly to the  $YK$ -axis) and the contour point in the origin. The  $YK,ZK$ -plane represents a differential sector out of the corresponding surface in the vicinity of the origin. Within the system  $(XQ,YQ,ZQ)$  (Fig. 2) the line charge starting in the origin will be placed on the  $ZQ$ -axis so that the calculation of potential  $P$  and fieldstrength  $E$  in any point will be simplified as far as possible. Each of the two auxiliary systems can occupy any position in the main system  $(X,Y,Z)$ , which is fixed by the site of its origin (shifting) and by the transformation determinant (rotation) [7]. Thus the input follows into the auxiliary coordinates  $(XK,YK,ZK)$  with subsequent transformation into the main system  $(X,Y,Z)$ . Potential and fieldstrength in a point are calculated so, that firstly the point will be transformed into the auxiliary system  $(XQ,YQ,ZQ)$  of each simulation charge. There the separate values will be calculated and after the reverse transformation into the main coordinates  $(X,Y,Z)$  added by superposition to the result. Therefore any spatial arrangement in the main system  $(X,Y,Z)$  can be described despite the strongly simplified geometry in the auxiliary systems.

### TYPES OF SIMULATION CHARGES

Different types of simulation charges are necessary to make possible an optimum adapting for the field which has to be calculated by minimum cal-



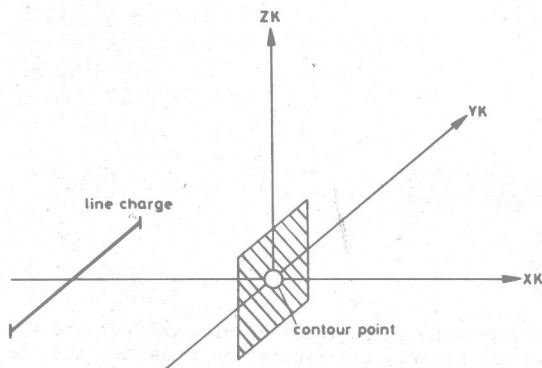


Fig. 1  
Auxiliary coordinates related  
to a contour point

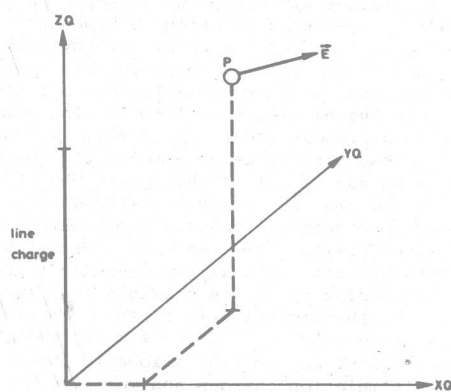


Fig. 2  
Auxiliary coordinates related  
to a simulation charge

calculation expense. According to their geometry they can be sectioned into three groups.

**Concentrated charges** - This type of simulation charge has the disadvantage, that at the position of the simulation charge itself potential and field strength become infinitely large owing to the infinite charge density. Therefore calculations close to or at these positions are not possible. As far as in those regions (e.g. inside of electrodes) no results are needed, concentrated charges may be used advantageously because of their low calculation expense. Using point-, finite line- and ring segment-charges has been proved as a sufficient variety of geometric forms [5].

**Area charges** - Area charges [6] may be used advantageously for the calculation of thin electrodes or surface charges. This type of charges allow calculations at the position of the charge too owing to the finite charge density. The calculation expense is larger than at concentrated charges, however, it is often possible to replace a larger number of concentrated charges by a single area charge.

**Volume charges** - Space charge fields are mostly investigated on the basis of fundamental geometrics [8]. Calculations in this field with the simulation charge method are possible by using volume charges, which allow the description of spatially distributed charges. The determination of potential and field strength outside and inside the charge volume is possible without problems, due to finite charge density. Overlapping of the charge volumes is permitted. The first step proposed is the application

of sphere charges with constant space charge density  $Q'''$ . Outside the sphere with the radius  $r_0$  analogous equations (1,2) for potential  $P$  and field strength  $E$  are valid as for point charges, while inside the sphere other equations (3,4) are valid.

$$P = \frac{Q'''}{3\epsilon} \cdot \frac{2r_0^3}{r} \quad (1) \quad E = \frac{Q'''}{3\epsilon} \cdot \frac{r_0^3}{r^2} \quad (2)$$

$$P = \frac{Q'''}{3\epsilon} \cdot \frac{1}{2} (5r_0^2 - r^2) \quad (3) \quad E = \frac{Q'''}{3\epsilon} \cdot r \quad (4)$$

The distribution of potential and field strength of a sphere charge is shown in Fig. 3 (dotted lines = point charge). Further volume charges (e.g. spheroids) may be developed for better adaption to any field geometries.

The use of complex electrical values for all types of simulation charges allows also the calculation of dephased potentials and field strengths.

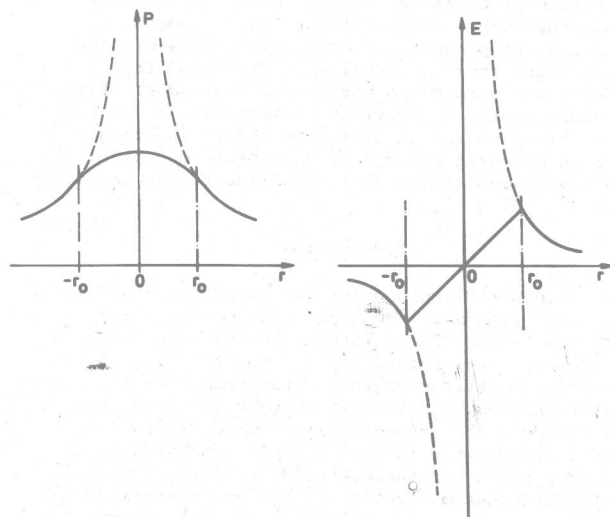


Fig. 3  
Potential and field strength of a sphere charge

#### INPUT CONDITIONS

By discretizing the physical arrangement into single simulation charges the field problem can be simplified to the determination of the unknown simulation charges ( $Q_1, Q_2, \dots$ ). Therefore it is only necessary to build up a linear equation system, which contains no further unknowns except simulation charges, so that the matrix can be kept small. For this equation system every physical condition for charges, field strengths or potentials may be used, which gives a linear relation between the simulation charges, as it is shown in the following examples:

**Fixed potential** - A given fixed potential  $P_j$  in a contour point yields the equation row  $j$

$$P_{1j}Q_1 + P_{2j}Q_2 + \dots = P_j \cdot 4\pi\epsilon_0 \quad (5)$$

where the potential coefficients  $p_{ij}$  describe pure geometry coefficients (due to the multiplication with  $4\pi\epsilon_0$ ).

**Free potential** - All contour points ( $m \dots n$ ) of an electrode on a free potential lead to one equation (5), whereby always the same but unknown potential of this electrode stands on the right side. This additional unknown can be eliminated by subtracting the equations of each other (e.g. row  $j$  - row  $k$ )

$$(p_{1j} - p_{1k})Q_1 + (p_{2j} - p_{2k})Q_2 + \dots = 0 \quad (6)$$

The still lacking additional equation row can be won either out of the known total charge  $\Sigma Q$  of the electrode

$$Q_n + Q_{n+1} + \dots + Q_m = \Sigma Q \quad (7)$$

or out of the given fieldstrength component (e.g. normal component) in one of the contour points  $m \dots n$  according to equation (8).

**Fixed fieldstrength component** - Linear relations between fieldstrength and simulation charges can not be set up in each case due to the vector nature of the fieldstrength. Giving an absolute value of fieldstrength is not possible in general, because it leads to a quadratic equation. It is often sufficient, to give any single fieldstrength component  $E_K$  especially if the other two components are known or without importance (e.g. the normal component  $E_N$  on an electrode surface, because the both tangential components are zero in this case). Every spatial direction is admissible for the given component. There results an equation row j

$$e_{1j}Q_1 + e_{2j}Q_2 + \dots = E_K \cdot 4\pi\epsilon_0 \quad (8)$$

in which  $E_K$  describes the given fieldstrength component and  $e_{ij}$  the geometric fieldstrength coefficient in direction of component  $E_K$ . Giving the complete fieldstrength vector  $\vec{E}$  by its components  $E_x, E_y, E_z$  is also possible in principle. But the three arising equation rows require three simulation charges, which should lie best on the three axis directions through the contour point. However, this is not possible in any case.

**Various dielectrics** - The simulation charge method assumes everywhere  $\epsilon = \epsilon_0$ . Nevertheless, various dielectrics can be reproduced with it, by arranging fictive surface charges at the boundary surfaces, which are represented by area charges [6] or alternatively valid simulation charges [2] at both sides of the boundary surface. Doing this the immediate relation between physical and calculated values of charges and flux densities is not given anymore. Potentials and fieldstrengths, however, are not influenced. The input condition (9) for the simulation charge is given by constant normal values (with any spatial direction) of the electric flux density ( $\epsilon_0 E_N$ ) at both sides of the boundary surface between the regions a and b corresponding to equation (8). Using alternatively valid simulation charges ( $Q_a$  is valid for the region b,  $Q_b$  for the region a) the continuance of potential in the contour point ( $P_a \equiv P_b$ ) will be used corresponding to equation (5) as a second input condition. The additional unknowns  $E_N$  and  $P_a \equiv P_b$  are eliminated again by subtraction resulting in the following equations:

$$(\epsilon_{ra} - \epsilon_{rb}) e_{1j}Q_1 + \dots - \epsilon_{rb} e_{ja}Q_a + \epsilon_{ra} e_{jb}Q_b \dots = 0 \quad (9)$$

$$Q_a Q_1 + \dots - p_a Q_a + p_b Q_b \dots = 0 \quad (10)$$

**Fixed Simulation Charges** - The input of known simulation charges does not require any new input condition. The values of these charges, however, have to be taken into account at all equations on the right side. Besides, they must be integrated into the calculation of results for potentials and fieldstrengths.

#### PARTICLE CHARGING IN IN UNIFORM FIELDS

The applied example is the charging process of particles with different form which is of interest for electrostatic precipitators or powder coating.

The conducting assumed particles may be charged on free potential in a homogenous field  $E_0$ . They are calculated first for the uncharged state ( $Q = 0$ ). By influence arises a symmetric electrical field with maximum absolute values  $E_{\max}$  at the vertices. Charge carriers in the proximity of particles are moving according to these field lines and charge the particles, as long as (at positive polarity) no field lines, coming from outside, end on the particle. The maximum charge  $Q_{\max}$  of the particle, then reached, can be calculated by setting the fieldstrength (component) in the upper vertex equal zero. An accordingly increased maximum fieldstrength  $E_{\max}$  arises in the lower vertex. As long as  $E_{\max}$  does not exceed the onset fieldstrength the theoretically calculated value  $Q_{\max}$  can be actually reached. In the other case the charging value remains lower. At negative polarity only the signs change, whereas the relations of the absolute values remain the same. The values for a conducting sphere with diameter  $d_K$  can be calculated analytically too. For the uncharged sphere ( $Q = 0$ ) results a maximum fieldstrength  $|E_{\max}| = 3 \cdot |E_0|$  at both vertices. At fully charged sphere the maximum fieldstrength in the lower vertex  $|E_{\max}| = 6 \cdot |E_0|$  and the maximum total charge of the sphere is

$$Q_K = 3\pi d_K^2 \epsilon_0 E_0 \quad (11)$$

For approximation calculations spheres with identical volume are used, independent from the actual form of particles. The actual deviations for cylindrical bodies with identical volume and half-spheres on both sides ( $d$  = diameter,  $h$  = height) were calculated numerically and presented in Fig. 4 and 5 and table 1. The fieldstrengths  $E_{\max}$  are related to the fieldstrength  $E_0$  of the homogenous field, and the maximum charge  $Q_{\max}$  of the bodies is related to the maximum charge  $Q_K$  of the sphere with identical volume corresponding to equation (11).

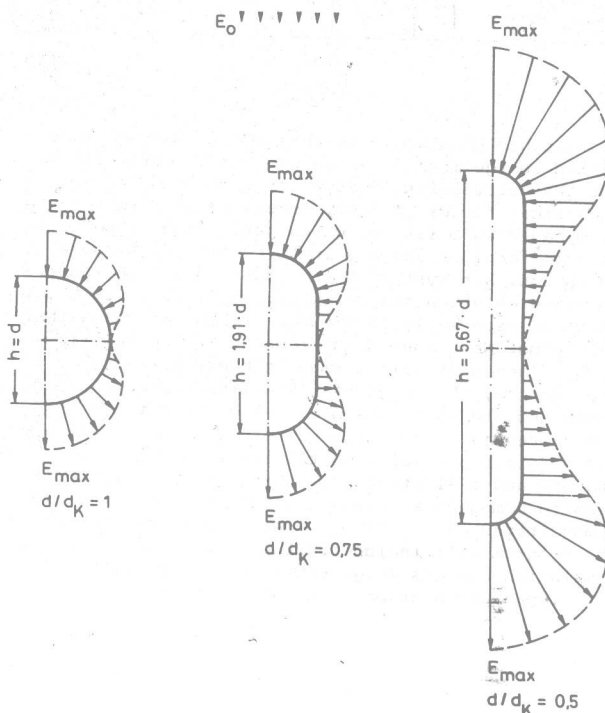


Fig. 4  
Uncharged bodies in homogenous field  $E_0$

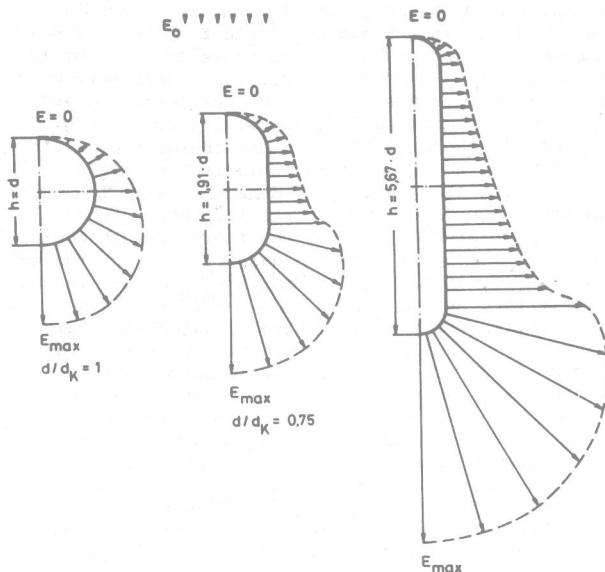


Fig. 5  
Full charged bodies in homogenous field  $E_0$

Table 1: Charging of particles with different forms						
$d/d_K$	1	0,9	0,8	0,7	0,6	0,5
$h/d$	1	1,25	1,64	2,28	3,42	5,67
$E_{max}/E_0 (Q=0)$	3	3,3	3,8	4,5	5,7	7,9
$E_{max}/E_0 (Q_{max})$	6	6,7	7,6	9,0	11,5	15,8
$Q_{max}/Q_K$	1	1,04	1,11	1,27	1,56	2,15

#### CONCLUSION

It has been shown in this paper that the simulation charge method can be used as an effective way for the calculation of asymmetric three-dimensional electrical fields. A newly developed computer program had been built up, which permits any type of simulation charges and any input conditions because of its strong kit system. Volume charges are introduced as new simulation charge types, which will yield advantages especially on the calculation of space charge fields. New input conditions allow the description of any spatially formed boundary surfaces of dielectrics, the input of fixed fieldstrength components and the calculation of charged electrodes on free potential. The influence of geometry of variously formed particles on the limiting values of charges and fieldstrengths during their charging process in homogenous fields has been investigated and demonstrated as an example. The future development of the program will include further input conditions and simulation charges (e.g. spheriods), a simplified data input and a graphic output of the results.

#### References

- [1] H.Steinbigler, Anfangsfeldstärken und Ausnutzungsfaktoren rotationssymmetrischer Elektrodenanordnungen in Luft. Dissertation TU München 1969
- [2] P.Weiß "Berechnung von Zweistoffdielektrika" ETZ-A, vol. 90, pp. 693 - 694, 1969.
- [3] B.Bachmann "Freies Potential beim Ladungsverfahren". ETZ-A, vol. 94, pp. 741 - 742, 1973.
- [4] H.Singer "Die Berechnung des elektrostatischen Feldes von Gittern". ETZ-A, vol. 91, pp. 249 - 253, 1970.
- [5] D.Utmischi, Das elektrische Feld unter Hochspannungsfreileitungen. Dissertation TU München, 1976.
- [6] H.Singer "Flächenladungen zur Feldberechnung von Hochspannungssystemen". Bull. SEV, vol. 65, pp. 739 - 746, 1974.
- [7] I.N. Bronstein and K.A. SEMENDJAJEW, Taschenbuch der Mathematik. Zürich und Frankfurt: Harri Deutsch, 1966, pp. 186 - 187.
- [8] E.U. Landers "Distribution of electrons and ions in a corona discharge". IEE Proc., vol. 125, pp. 1069 - 1073, Okt. 1978.





ELECTRIC FIELD CALCULATION IN 2 DIMENSIONAL MULTIPLE  
DIELECTRIC BY THE USE OF ELLIPTIC CYLINDER CHARGE

S. Sato, S. Menju, K. Aoyagi and M. Honda

Toshiba Corporation, Kawasaki, Japan

ABSTRACT

In this paper, 2-dimensional field analysis is investigated using elliptic cylinder charge in advanced charge simulation method. It has been clarified that not only the field of a single dielectric can be analyzed with high precision, but also those of multiple dielectrics and electrode with no thickness can be done easily only by elliptic cylinder charge.

INTRODUCTION

Electric field analysis provides important roles for the development of design and analysis of high-voltage apparatus, as well as the analysis of various discharge phenomena. It has recently made remarkable progress by C.S.M. (the charge simulation method), S.S.M. (the surface charge simulation method) [1], and F.E.M. (the finite element method).

C.S.M. especially features its high-speed and high-precision calculation but is said to be capable of calculating two different dielectric at the most, without special dielectrics techniques such as successive image method.

On the contrary, S.S.M. can analysis any types of multiple dielectric fields but involves unavoidable disadvantages in both computational precision and time because the digital integration in the process of calculating coefficients of electric potential and field is essential to it.

The third method, F.E.M., is especially suitable for analysis of fields having complicated boundary configuration, and is capable of processing multiple dielectrics of nonlinear characteristics. However, low precision is its vital drawback in general.

The authors have successfully developed a new method for analyzing multiple dielectric and electrodes without thickness that could not be analyzed by the method up to this day. This method uses formula of charges obtained by the direct solution of the Laplace's equation[2] and it has the merits of both C.S.M. and S.S.M.

MULTIPLE DIELECTRIC CONCEPTION

A multiple dielectric field is calculated by the similar method to the conception of S.S.M.

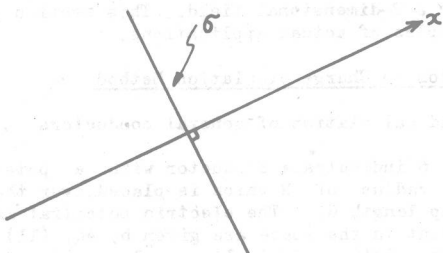


Fig. 1 A plate charge

See Fig. 1. If a plate charge with a surface charge density  $\sigma$  exists in any position of the space, the electric potential and the field along direction

perpendicular to the charge are assumed as shown in Fig. 2 (a) and (b), respectively.

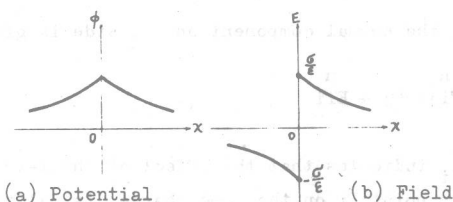


Fig. 2 Potential and field distribution through the plate charge

Characteristic of these two curves satisfy the nature like the electromagnetic condition on the dielectric boundary, namely,

- (a) The potential is continuous along the path through the plate charge.
- (b) The normal (x) components of the field are not continuous and have opposite signs on both sides of the charge.

The concept of S.S.M. is that lots of surface charges are used to turn the condition (b) as to satisfy the condition for the boundary of dielectrics.

In Fig. 3, the following two electromagnetic conditions (c) and (d) should be satisfied on the boundary B whose relative permittivities are  $\epsilon_1$  and  $\epsilon_2$  on both sides.

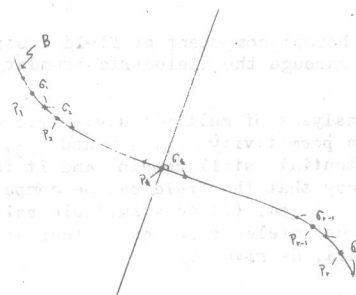


Fig. 3 Plate charges pasted on the boundary

- (c) The potential is continuous or the tangential components of the field are equal to each other.

$$\phi_1 = \phi_2 \text{ or } E_{1t} = E_{2t} \quad (1)$$

- (d) The normal components of the electric flux density are equal to each other.

$$D_{1n} = D_{2n} \text{ or } \epsilon_1 E_{1n} = \epsilon_2 E_{2n} \quad (2)$$

If the boundary B is divided into r-sections, and plate charges of charge density  $\sigma_j$  ( $j = 1 - r$ ) are pasted on each section then the potential at point Pk on the k-th charge from a superposition of the potential of k-th